Metallurgical Mechanisms Controlling Mechanical Properties of Aluminum Alloy 2219 Produced By Electron Beam Freeform Fabrication

Marcia S. Domack[a], Karen M. B. Taminger[b], and Matthew Begley

NASA Langley Research Center, Mail Stop 188A, Hampton, VA, USA 23681
[a]Marcia.S.Domack@nasa.gov, [b]Karen.M.Taminger@nasa.gov

Keywords: Aluminum alloy 2219, electron beam deposition, mechanical properties, microstructural analysis

Abstract. The electron beam freeform fabrication (EBF^3) layer-additive manufacturing process has been developed to directly fabricate complex geometry components. EBF^3 introduces metal wire into a molten pool created on the surface of a substrate by a focused electron beam. Part geometry is achieved by translating the substrate with respect to the beam to build the part one layer at a time. Tensile properties have been demonstrated for electron beam deposited aluminum and titanium alloys that are comparable to wrought products, although the microstructures of the deposits exhibit features more typical of cast material. Understanding the metallurgical mechanisms controlling mechanical properties is essential to maximizing application of the EBF^3 process. In the current study, mechanical properties and resulting microstructures were examined for aluminum alloy 2219 fabricated over a range of EBF^3 process variables. Material performance was evaluated based on tensile properties and results were compared with properties of Al 2219 wrought products. Unique microstructures were observed within the deposited layers and at interlayer boundaries, which varied within the deposit height due to microstructural evolution associated with the complex thermal history experienced during subsequent layer deposition. Microstructures exhibited irregularly shaped grains, typically with interior dendritic structures, which were described based on overall grain size, morphology, distribution, and dendrite spacing, and were correlated with deposition parameters. Fracture features were compared with microstructural elements to define fracture paths and aid in definition of basic processing-microstructure-property correlations.

Introduction

The electron beam freeform fabrication (EBF^3) process has been developed at NASA Langley Research Center to directly fabricate complex geometry components, add structural details to manufactured pre-forms, and enable development of novel graded property materials.[1] The EBF^3 process introduces metal wire into a molten pool created on the surface of a substrate by a focused electron beam. Part geometry is achieved by translating the substrate with respect to the beam to build the part one layer at a time.

Tensile properties have been demonstrated for electron beam deposited aluminum and titanium alloys that are comparable to wrought products.[2, 3] The mechanical properties of as deposited Al 2219 material were between typical values for sheet and plate in the annealed (O) and naturally aged (T4) tempers.[2] Deposits of Al 2219 heat treated to the T6 temper exhibited properties nearly equivalent to typical T62 handbook values for sheet and plate products.[2] While mechanical properties were similar, the microstructures of the deposits exhibited features more typical of cast material rather than those associated with wrought products.

In order to maximize application of the EBF^3 process it is essential to understand the metallurgical mechanisms controlling mechanical properties in deposited material. The current study examines the mechanical properties and resulting microstructures of aluminum alloy 2219 deposits fabricated using the EBF^3 system at NASA Langley for a range of process variables, including translation speed, wire feed rate, and beam power. Material performance was evaluated based on tensile properties, including ultimate tensile strength, yield strength, and percent total

elongation. Results were compared with published results for Al 2219 to evaluate process repeatability and were correlated with fracture features and microstructural elements.

Material

Deposits were fabricated using 2.3 mm diameter aluminum alloy 2319 wire. Al 2319 is commonly used as the filler wire in welding Al 2219, a commercially available aerospace alloy that is weldable and has good strength and toughness over a wide temperature range [4]. The measured composition of the Al 2319 wire used in this study was nominally Al – 6.1Cu – 0.30Mn - 0.01Mg – 0.12Zr - 0.09V – 0.13Ti – 0.13Fe - 0.04Si. The composition is identical to Al 2219 with the exception of increased level of Ti in Al 2319 to account for losses experienced during welding. For the purposes of this report, the electron beam deposits will be referred to as Al 2219 to facilitate comparison of the deposit properties with Al 2219 wrought products.

Linear deposits were fabricated on 6.4 mm thick Al 2219 base plates, as shown in Fig. 1. Deposits for metallurgical analysis and longitudinal orientation tensile specimens were one pass wide, nominally 25.4 cm long, 2.54 cm high, and 5 mm to 10 mm thick. Additional deposits for transverse orientation tensile specimens were one pass wide, nominally 25.4 cm long, 12.7 cm high and 10 mm thick. Process variables were adjusted to vary both the rate of material deposited and the energy input to the deposit (Table 1). The beam current and accelerating voltage were held constant while translation speed and wire feed rate were varied. Compared with the baseline A6 deposition parameters, wire feed was doubled for the A1 deposits while translation speed was doubled for the A6m deposits. The parameters resulted in high (A1), medium (A6), and low (A6m) deposition rates (Table 1), expressed as unit deposition volume and defined as the volume of wire deposited per unit length of the build. Since the beam output energy was held constant, the level of energy input per unit length of deposit varied with translation speed. By varying the wire feed rate, the parameter combinations resulted in two levels of energy input per unit volume (Table 1).

Table 1. Process parameters for the Al 2219 deposits.

Parameter	Deposit		
	A1	A6	A6m
Unit Deposition Volume, cm^3/cm	0.308	0.154	0.077
Energy per Unit Volume, $KJoule/cm^3$	254	532	532

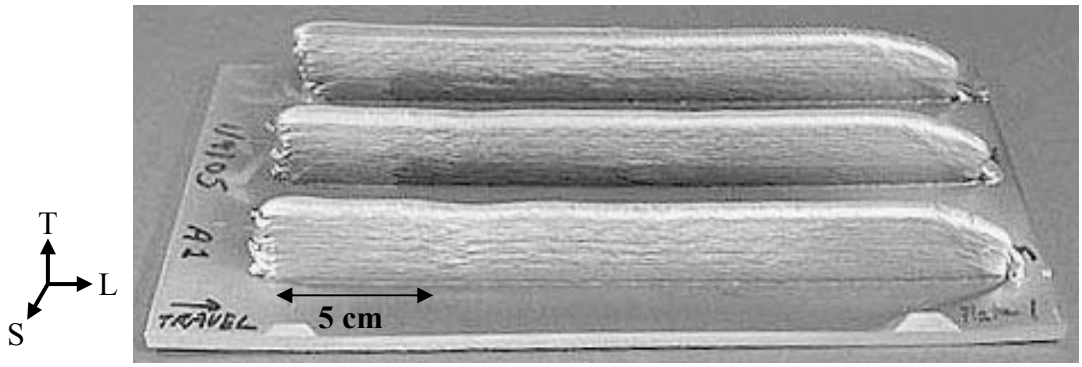

Figure 1. Typical Al 2219 deposit and defined coordinate system.

Procedures

A coordinate system defined for the deposits is shown in Fig. 1, where the longitudinal direction (L) was defined to be parallel to the base plate translation (travel) direction, the long transverse direction (T) normal to the surface of the base plate, and the short transverse direction (S) across the width of the deposited layer. Tensile properties at room temperature were determined using standard 10 cm sub-size dog bone specimens in accordance with ASTM E8 [5].

Flat tensile specimens were machined in the LT plane and tested in the L direction for each set of deposition parameters and also in the T orientation for the A1 deposition parameters. In all cases the specimen thickness was approximately equal to the deposit width, with the surfaces machined flat and parallel to remove surface irregularities introduced by the EBF^3 process. Duplicate tensile specimens were tested in the as-deposited condition and after heat treatment to a T62 temper using a standard heat treatment schedule (solutionized at 535°C for one hour, cold water quench, and aged at 190°C for 36 hours [4]).

Results and Discussion

Tensile properties of the deposited material varied little over the range of deposition parameters used and were comparable to handbook values for similar gage wrought products. Yield and tensile strengths for the as-deposited materials (Fig. 2) were between typical values for annealed (O temper) and naturally aged (T4 temper) sheet and plate. Elongation values were similar or slightly less than for annealed products. Following heat treatment to a T6 temper, strength and elongation were nearly equivalent to wrought products in the T62 temper (Fig. 3). Yield and tensile strengths varied by less than two percent over the range of deposition parameters used, for both as-deposited and heat treated deposits. Elongation values were 10-15% higher for

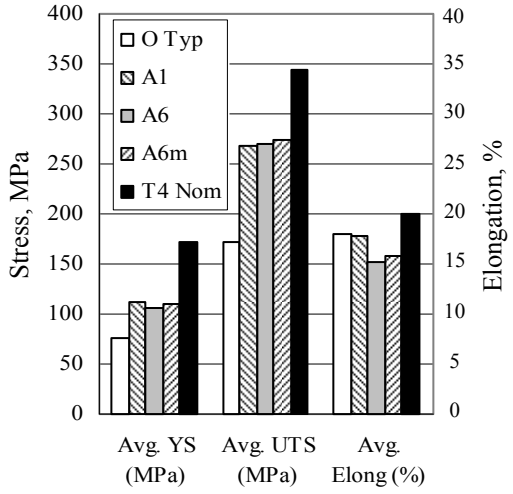

Figure 2. Tensile properties of as-deposited Al 2219 compared with Al 2219 wrought products in annealed (O) and naturally aged (T4) tempers [4].

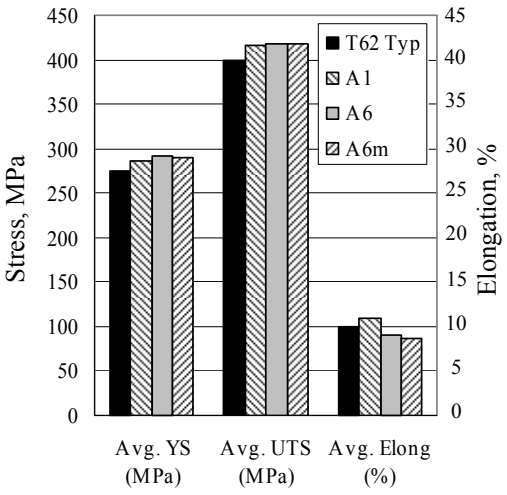

Figure 3. Tensile properties of heat treated Al 2219 deposits compared with Al 2219 wrought products in the T62 condition [4].

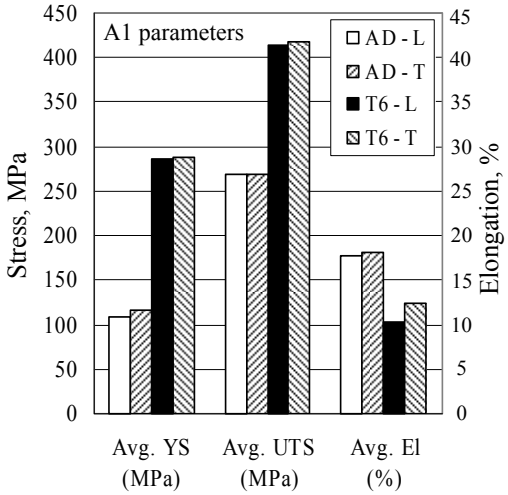

Figure 4. Isotropic tensile properties demonstrated for Al 2219 as-deposited (AD) and in T6 temper.

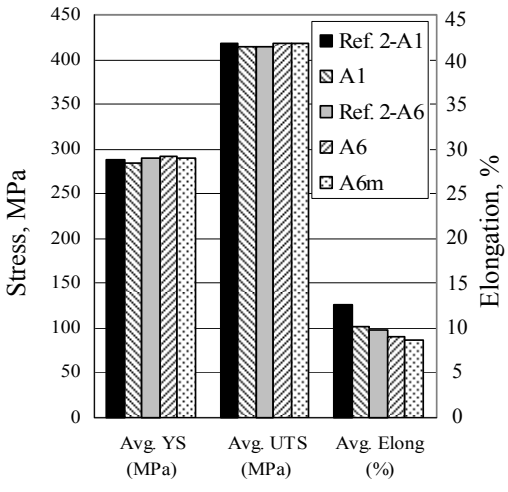

Figure 5. Tensile properties of Al 2219 comparable to published values in T6 [2].

the A1 parameters compared with deposits produced using the A6 or A6m parameters. Tensile properties were isotropic, as shown in Fig. 4 for the A1 parameters, with strength and elongation varying by less than two percent between L and T orientations for both as-deposited (AD) and T6 conditions. The properties of the deposits generated during the current study, averaged over all of the deposition parameters, were comparable to prior published results (Fig. 5) although elongation was somewhat lower for the A1 parameters in material deposited in the current study.[2]

Metallurgical cross sections prepared of the ST plane revealed variations in the macroscopic geometry and microstructural condition of the deposits. Deposit widths were approximately 0.94 cm for A1, 0.91 cm for A6, and 0.67 cm for A6m parameters, indicating that deposit width is controlled by the translation speed. Translation speed was the same for A1 and A6, but increased by a factor of two for the A6m deposits, resulting in 30% reduction in width. Distinct bands visible between deposited layers revealed that layer thicknesses were approximately 5 mm for A1, 2.3 mm for A6, and 1.3 mm for A6m, reflecting decreases proportional to the reductions in deposition volume from A1 to A6 to A6m (Table 1). The correlations between translation speed and deposit width and between deposition volume and layer thickness are consistent with prior observations.[2]

The microstructures throughout the bulk of the deposits were generally characterized by two grain types, with their distribution the primary variation with deposition parameters. As-deposited microstructures were dominated by irregularly shaped grains, with dimensions from 100 μm to 200 μm, which exhibited internal dendritic solidification structure (Fig. 6). Regions of smaller equiaxed grains, approximately 10 μm to 25 μm in diameter (Fig. 6), were spaced at intervals that corresponded to interlayer boundaries. The small grains regions were distributed in distinct bands in the A1 and A6m deposits (Fig. 7) but in less well developed bands in the A6 deposits. The interdendritic spacing appeared constant regardless of grain size (Fig. 8) or deposition parameters. Also noted was a semi-continuous grain boundary phase (light grey in Fig. 9), representing the Al-Cu eutectic composition, and needle-like Fe and Si bearing precipitates [6, 7]. The similarity in microstructures of all deposits suggests that microstructural evolution was controlled by solidification rates, which were similar regardless of energy input per unit volume.

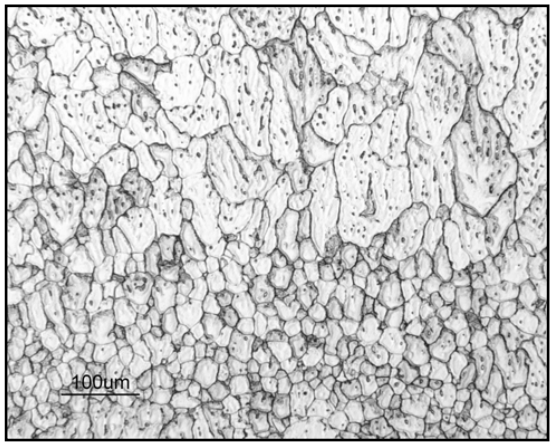

Figure 6. Representative grain morphology of as-deposited Al 2219.

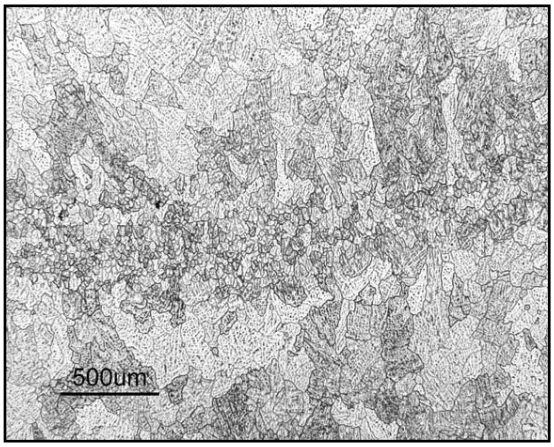

Figure 7. Small equiaxed grains at interlayer boundaries in as-deposited Al 2219.

Microstructures in the top (last) layer deposited exhibited equiaxed grains, approximately 200 μm to 500 μm in diameter, with coarse internal dendritic structures and undefined grain boundaries. Comparison with the bulk microstructures indicated that re-melting, grain refinement, and constituent homogenization occurred during deposition of subsequent layers. Microstructures in the first layers deposited exhibited large, elongated grains with dimensions from 200 μm to over 1000 μm, with internal structure similar to the bulk of the deposits, but with elongated dendrites at the interlayer boundaries. The base plate likely provided a heat sink sufficient to affect the thermal profile in the first layers deposited with steady state conditions developing in the bulk.

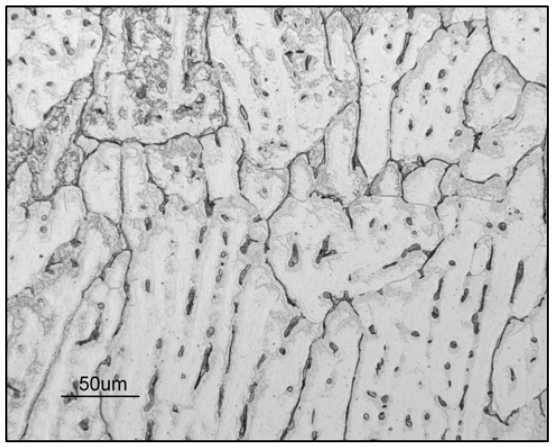

Figure 8. Dendritic structure typical for irregular and equiaxed grains in as-deposited Al 2219.

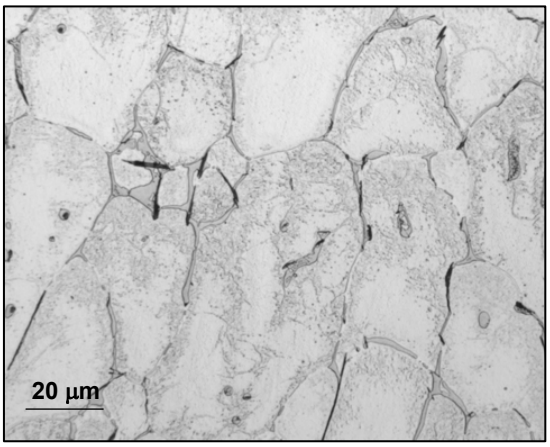

Figure 9. Grain boundary eutectic phase and Fe, Si precipitates in as-deposited Al 2219.

Following heat treatment to a T62 temper, the microstructures retained the prior grain boundaries and, consequently, the duplex grain sizes, but exhibited transformed internal dendritic structures (Fig. 10). The interior structure was globular, refined, and based on response to etching, exhibited a further homogenization of constituent distribution. The grain boundary eutectic phases were largely dissolved but the needle-like Fe, Si precipitates were retained (Fig. 11).

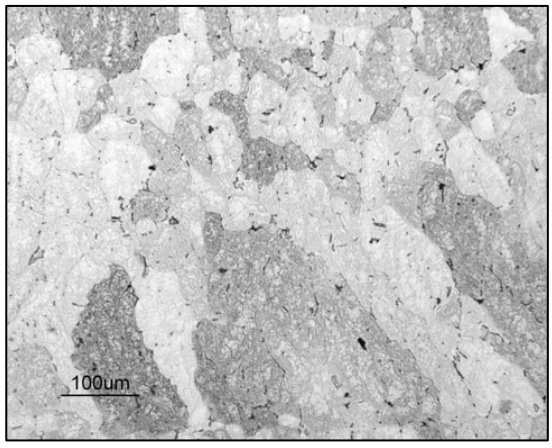

Figure 10. Representative grain morphology of Al 2219 deposits following T6 heat treatment.

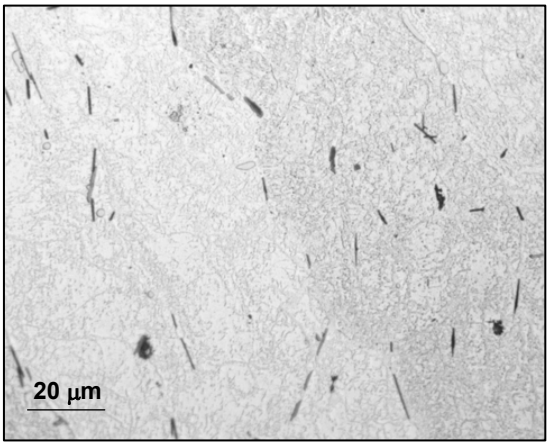

Figure 11. Transformed internal dendritic structure following T6 heat treatment.

Fracture morphology was transgranular for all of the deposition parameters and material conditions. Fracture surfaces from tensile samples tested in the as-deposited condition exhibited two primary fracture features, shallow dimples and regions exhibiting low ductility lamellar features (Fig. 12). For the A1 and A6m deposits, the dimpled and lamellar regions were distributed in distinct bands that correlated with the distribution of grain sizes observed in the metallurgical samples (Fig. 12a). For the A6 deposits, the shallow dimples were distributed in clusters rather than well defined bands, as was observed in the microstructure. The size of the dimples and the size and separation of lamellar features were consistent with the size of the small equiaxed grains and the scale of the dendritic structure observed in the microstructures (Fig. 12b).

Following heat treatment to the T62 temper, the fracture morphology was transgranular ductile rupture characterized by shallow dimples of two sizes (Fig. 13a). Fracture was dominated by regions of very fine dimples (Fig. 13b), reflecting transgranular fracture of the transformed internal dendritic microstructure. Scattered regions of dimples approx. 10 μm in diameter reflected fracture through the small equiaxed grains. The distribution of fracture features was similar for all of the deposition parameters after heat treatment to the T6 condition. The transgranular fracture morphology was similar to that typically observed in Al 2219 wrought products.

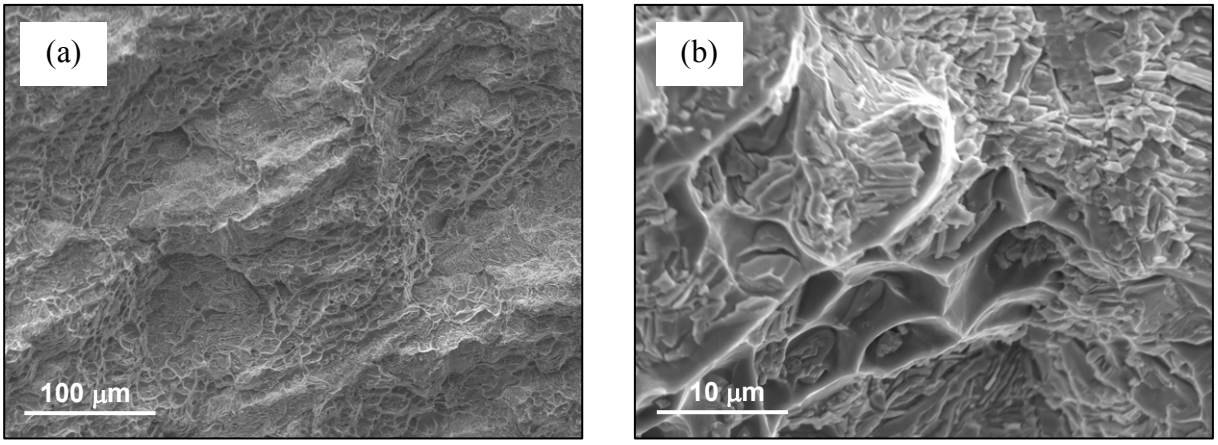

Figure 12. Representative distribution (a) and scale (b) of shallow dimples and lamellar features observed on fracture surfaces of as-deposited Al 2219 material.

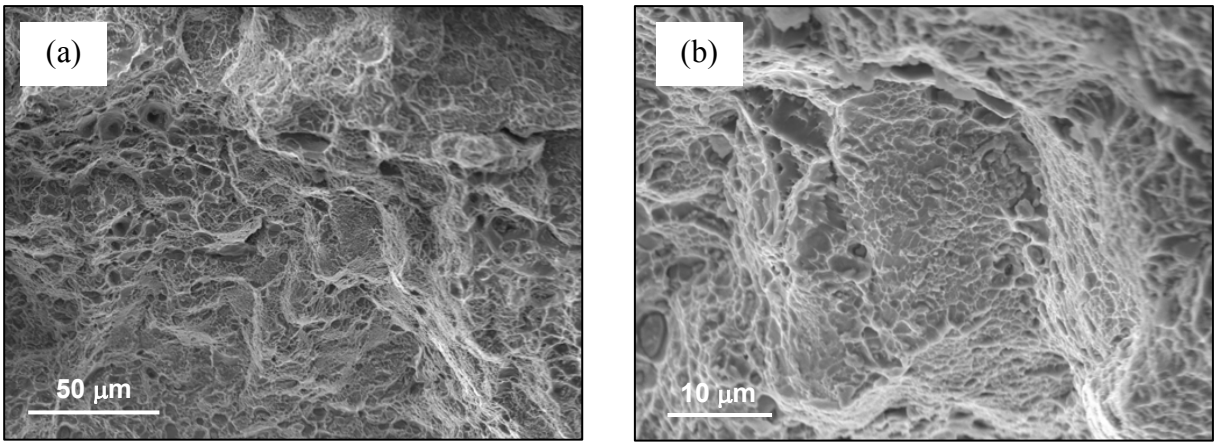

Figure 13. Representative distribution (a) and scale (b) of shallow dimples observed on fracture surfaces of deposited Al 2219 material.

Summary

Deposits of aluminum alloy 2219 built using the electron beam freeform fabrication (EBF^3) process were evaluated to correlate tensile mechanical properties with microstructure and fracture features. Tensile mechanical properties for both as-deposited and T6 temper deposits were in good agreement with published values for wrought products and were constant regardless of deposition parameters. The width of the deposits was controlled by translation speed and the thickness of individual layers by deposition rate. Microstructures of the as-deposited materials were similar for the deposition parameters, exhibiting grains with internal solidification structures with grain refinement at interlayer boundaries. Microstructural refinement occurred during deposition of subsequent layers. Fracture of as-deposited material occurred by low ductility transgranular fracture along dendrite boundaries and through the refined grains. Heat treatment to T6 temper transformed and refined the dendritic structure and homogenized constituent distribution. Fracture of T6 temper deposits occurred by transgranular ductile rupture uniformly through the grain structure with limited fracture through refined grains.

References

[1] K. M. Taminger and R. A. Hafley: 3rd Annual Automotive Composites Conference, 2003.
[2] K. M. Taminger and R. A. Hafley: 13th Solid Freeform Fabrication Symposium (SFF), 2002.
[3] T. Wallace, K. Bey, K. Taminger and R. Hafley: 15th SFF (2004). pp. 104-115.
[4] L. W. Mayer, *Alcoa Green Letter: Alcoa Aluminum Alloy 2219* (1967).
[5] Annual Book of ATSM Standards, E8-96 (1996), vol. 3.01, pp. 55-76.
[6] Metallography and Microstructures, ASM Handbook, Vol. 9, p. 107, 711.
[7] Aluminum – Properties and Physical Metallurgy, p. 70.